PHYSICAL REVIEW B **90**, 155128 (2014)

Electrical transport properties of CaB_6

Jolanta Stankiewicz,[1,*] Javier Sesé,[2] Geetha Balakrishnan,[3] and Zachary Fisk[4]
[1]*Instituto de Ciencia de Materiales de Aragón and Departamento de Física de la Materia Condensada, CSIC–Universidad de Zaragoza, 50009-Zaragoza, Spain*
[2]*Instituto de Nanociencia de Aragón and Departamento de Física de la Materia Condensada, Universidad de Zaragoza, 50018-Zaragoza, Spain*
[3]*Department of Physics, University of Warwick, Gibbet Hill Road, Coventry CV4 7AL, United Kingdom*
[4]*Department of Physics and Astronomy, University of California, Irvine, California 92697, USA*
(Received 25 August 2014; revised manuscript received 3 October 2014; published 24 October 2014)

We report results from a systematic electron-transport study in a broad temperature range on 12 CaB_6 single crystals. None of the crystals were intentionally doped. The different carrier densities observed presumably arise from slight variations in the Ca:B stoichiometry. In these crystals, the variation of the electrical resistivity and of the Hall effect with temperature can be consistently accounted for by the model we propose, in which B-antisite defects (B atom replacing Ca atom) are "amphoteric." The magnetotransport measurements reveal that most of the samples we have studied are close to a metal-insulator transition at low temperatures. The magnetoresistance changes smoothly from negative—for weakly metallic samples—to positive values—for samples in a localized regime.

DOI: 10.1103/PhysRevB.90.155128 PACS number(s): 72.20.My, 72.15.Rn, 71.55.Ht

I. INTRODUCTION

Alkaline- and rare-earth hexaborides have been the focus of extensive experimental and theoretical studies for over four decades. This continuing interest is coming from the diversity exhibited throughout this class of materials. Unusually small changes in the band configuration tend to lead to profound alterations of the physical properties of these systems. Much recent interest in alkaline-earth hexaborides is brought about by the discovery of an uncommon type of ferromagnetism in CaB_6 [1] and SrB_6 [2] more than a decade ago. The long-range ordering to a Curie temperature of 600 K was unexpected because these compounds do not have partially occupied $3d$ or $4f$ orbitals. Extensive theoretical and experimental research of the electronic properties of CaB_6 has not, however, led to a clear explanation of the observed ferromagnetism. This was exhaustively reviewed by Edwards and Katsnelson [3]. Furthermore, an overall picture of electronic transport in alkaline-earth hexaborides is missing as well. Experiments performed to date on CaB_6 have produced many unclear results. Contradictory effects are observed even in crystals nominally with the same stoichiometry. The goal of this paper is to fill this gap. Through systematic study of different single crystals, we establish general features of electronic transport in calcium hexaboride, and comprehensively model them.

The CaB_6 system crystallizes in a simple cubic structure which can be pictured as a CsCl arrangement of B_6 octahedra and alkaline-earth atoms. The boron network requires two electrons to form a closed shell configuration; therefore, binary alkaline-earth hexaborides are semiconductors. This has been corroborated by angle-resolved photoemission spectroscopy experiments and by a GW calculation, which confirms the existence of an energy gap of about 0.8 ∓ 0.1 eV at the X point in the Brillouin zone [4]. At the same time, alkaline-earth hexaborides are prone to the formation of defects. Thermopower and resistivity data suggest that the native defects are mainly donors, because the itinerant charge carriers are electrons [5,6]. These, most likely, are metal vacancies or unintentional impurities, as shown by various studies of CaB_6 and SrB_6 [7–9]. Close to the stoichiometric composition, CaB_6 exhibits quasisemiconducting behavior in an extended temperature range [8]. At lower temperatures, its behavior is rather complicated and seems to be sample dependent.

In this paper, we present results of a systematic electron transport study on 12 different CaB_6 single-crystal samples. None of them were intentionally doped. The different carrier densities we have observed presumably arise from slight variations in the Ca:B stoichiometry. The variation of the electrical resistivity and of the Hall effect with temperature in these crystals can be consistently accounted for by a model we propose, in which B-antisite defects (a B atom replaces a Ca atom) are "amphoteric." Most of the samples we have studied are close to a metal-insulator transition at low temperatures. This is unveiled by our magnetoresistance measurements, in which we find that the magnetoresistance changes smoothly from negative—for weakly metallic samples—to positive values—for samples in a localized regime.

II. EXPERIMENT

The single crystals of CaB_6 used in our study were grown from Al flux with no intentional doping. The starting materials were 6N (99.9999% purity) boron, 3N calcium (99.98% purity), and 3N aluminum for crystals prepared at Irvine. Boron powder of 99% purity, 4N Ca pieces, and 3N Al were used at Warwick. Almost all materials proceeded from Alfa Aesar or Sigma Aldrich. The CaB_6 crystals appeared to contain vacancies on calcium sites. These gave rise to a certain degree of self-doping. All CaB_6 samples grown at Warwick contained, in addition, an appreciable amount of unidentified donors, most likely coming from boron powder. The crystals had the form of thin platelets or prisms. All measurements were performed on small single crystals of approximately $0.2 \times 0.5 \times 3$ mm^3.

*jolanta@unizar.es

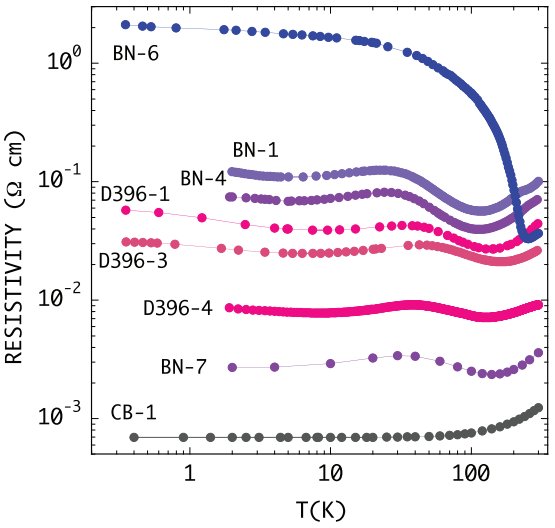

FIG. 1. (Color online) Variation of electrical resistivity with temperature for various stoichiometric CaB_6 single crystals.

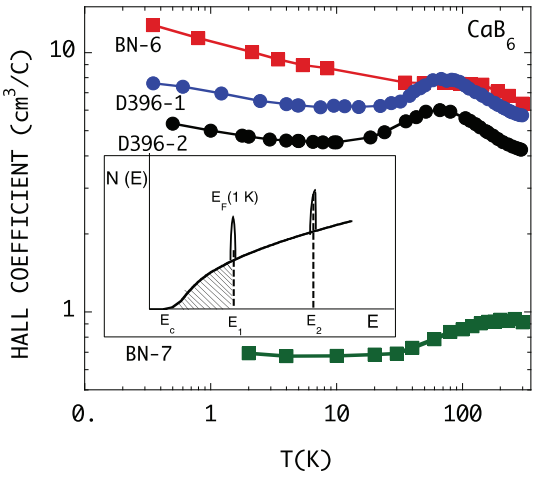

FIG. 2. (Color online) Variation of Hall coefficient with temperature for various stoichiometric CaB_6 single crystals. The inset schematically shows the density of states vs energy in our model.

Prior to experiments, the crystals were cleaved and polished using polishing films with diamond particles. Surfaces were cleaned by etching them in concentrated HCl acid. Low frequency transport measurements were carried out in helium cryostats with a six-probe method. We used pure indium or silver paint in order to attach—on previously deposited gold spots—contact leads (25 μm gold wire) to the samples. In some cases, the contacts were spot welded. The Hall resistivity was measured as a function of the magnetic field: (1) in the $(-1,1)$ T range, for temperatures above 10 K, and (2) up to 10 T, at low temperatures. The magnetization measurements in the 2–300 K temperature range and in magnetic fields of up to 5 T were made using a commercial superconducting quantum interference device magnetometer. We have used the same crystals in electrical transport and magnetic measurements.

III. RESULTS AND DISCUSSION

How the electrical resistivity varies with temperature in stoichiometric CaB_6 single crystals is shown in Fig. 1. Overall, the resistivity $\rho(T)$ in all samples, except in the purest one, has a rather weaker temperature dependence than would be expected for an undoped semiconductor. Upon lowering the temperature from 300 K, $\rho(T)$ first decreases, showing a broad minimum at about 120 K, and subsequently increases. The resistivity may show another broad minimum at approximately 10 K and increase beyond that point. The Hall resistivity for these samples varies linearly with the magnetic field and shows a negative slope, which implies a predominantly electron-type conduction. The temperature variation of the Hall coefficient, R_H, plotted in Fig. 2, is atypical: It shows a broad maximum around 100 K. This cannot be accounted for by a two-carrier model. We note that the variation seen in the Hall and resistivity data from sample to sample is quite large, even for crystals from the same batch. Accordingly, we decided to characterize each sample individually. Their conductivities and carrier concentrations at 2 and 295 K are given in Table I.

To explain our results, we assume that some intrinsic defects, most likely boron atoms at the Ca^{+2} vacancy sites, have charges which may vary from $+1$ to -1 with respect to the Ca^{+2} lattice. This is supported by observations that (i) stoichiometrically grown CaB_6 has vacancies on the calcium sites [10]; (ii) the formation of B antisites (B_{Ca}) is a principal defect in Ca-deficient CaB_6 [11]; and (iii) Ca and B atoms have two and three valence electrons, respectively; therefore, B_{Ca} can exist in three charge conditions: $+1$, 0, and -1 with respect to the Ca sublattice (B ion as B^{+3}, B^{+2}, and B^{+1}). This implies that—depending on the location of the Fermi energy—these defects can either act as acceptors or as donors. In addition, if they are highly localized, their energy levels will be correlated neither with the positions of the conduction band nor with any valence band edges. Thus, the energy levels of these defects can be located anywhere within the gap or even in the conduction band [12].

The treatment of several energy levels of the same defect atom calls for the use of the Gibbs distribution [13,14]. Therefore, for B_{Ca} we have (see a sketch in Fig. 2)

$$A(g_0' + g_1' e^{-(E_1-E_F)/k_BT} + g_2' e^{-(E_2-2E_F)/k_BT}) = 1, \qquad (1)$$

TABLE I. Transport parameters obtained for CaB_6 single crystals from resistivity and Hall effect measurements.

Sample	n (2 K) (cm^{-3})	σ (2 K) $(\Omega\,cm)^{-1}$	n (295 K) (cm^{-3})	σ (295 K) $(\Omega\,cm)^{-1}$
BN-1	7.17×10^{17}	8.26		9.90
BN-2	8.80×10^{17}	18.50		10.00
BN-3	3.10×10^{17}	1.26	1.25×10^{18}	37.90
BN-4	5.80×10^{17}	13.30		14.20
BN-5	5.15×10^{17}	8.48		10.53
BN-6	6.20×10^{17}	0.53	9.75×10^{17}	27.03
BN-7	9.10×10^{18}	370.3	6.84×10^{18}	277.8
D396-1	9.61×10^{17}	23.01	1.09×10^{18}	22.60
D396-2	1.32×10^{18}	25.60	1.48×10^{18}	35.21
D396-3	1.65×10^{18}	36.50		38.02
D396-4	5.25×10^{18}	116.3		109.9
CB-1	3.37×10^{19}	1440	3.38×10^{19}	810.0

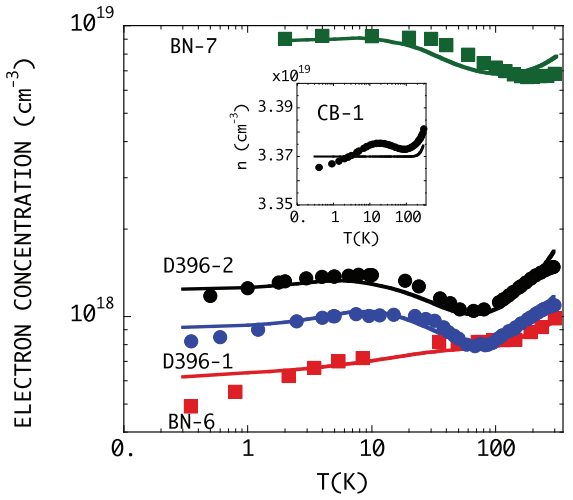

FIG. 3. (Color online) Electron concentration vs temperature for various CaB_6 single-crystal samples. Solid lines are fits to experimental data points using the model we propose here. The inset shows the same for the sample with high impurity concentration.

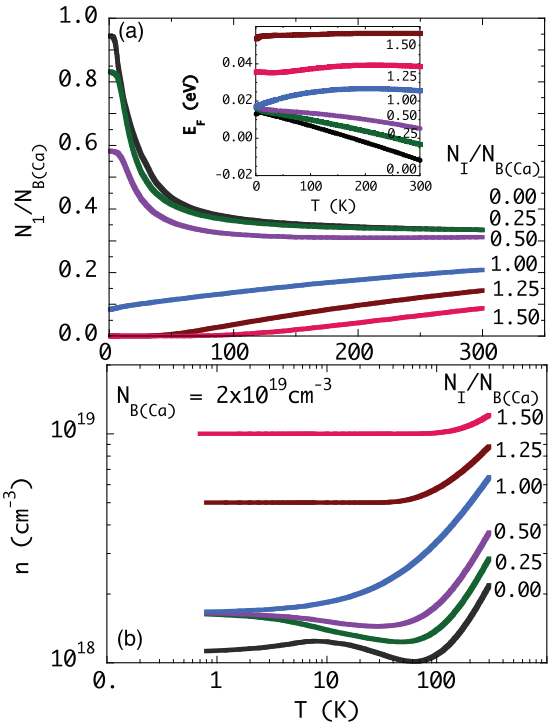

FIG. 4. (Color online) (a) The fraction of occupied E_1 defects vs temperature for various doping levels is shown. The inset shows the Fermi energy vs temperature. (b) Electron concentration vs temperature in the conduction band for various doping levels.

where $g_i' = g_i e^{S_i/k_B}$. $\{g_i\}$ is the set of statistical weights for states $i = 0$, 1 and 2, corresponding to the B ion with no electron, with one electron, and with two electrons, respectively; S_i is the vibrational entropy of these states; E_1 and E_2 are the energies of one and two electrons, respectively, at the defect, and E_F is the energy of the Fermi level with respect to the bottom of the conduction band. A and k_B are the normalization coefficient and Boltzmann constant, respectively. The electron concentration, $n(E_F,T)$, in the conduction band satisfies the neutrality condition:

$$n + (N_A - N_D) = N_{B_{Ca}} A(g_0' - g_2' e^{-(E_2-2E_F)/k_B T}), \qquad (2)$$

where $N_{B_{Ca}}$, N_A, and N_D are the concentrations of B-antisite defects, and of additional acceptor and donor impurities, respectively. Here, we assume the hole concentration in the valence band is negligible. We fit Eq. (2) to our Hall data with E_1, E_2, $N_{B_{Ca}}$, and $N_I = (N_D - N_A)$ as fitting parameters. $n(E_F,T)$ is obtained from numerical integration of the standard density-of-states expression for a parabolic band. We use $0.28m_0$ [15], where m_0 is the free electron mass, for the effective mass of the conduction electrons. Furthermore, $g_0 = 1$, $g_1 = 2$, and $g_2 = 1$. Assuming a very small ($\approx 10^{-4}$ eV/K for the E_1 state and 10^{-5} eV/K for the E_2 state) entropy content [8], we found that the values of $\simeq 0.013$ and 0.03 eV for E_1 and E_2, respectively, give the best fit to the measured ($n = 1/eR_H$) electron concentration in various CaB_6 single crystals. This is shown in Fig. 3. Our calculations reproduce rather well the observed experimental features, such as the minimum in $n(T)$ at about 100 K and a weak downturn below 10 K. The fit to the concentration of antisite defects varies from $\sim 6 \times 10^{17}$ cm^{-3}, for the BN-6 sample, to $\sim 1 \times 10^{19}$ cm^{-3} for CB-1, while the values of N_I are lower than $N_{B_{Ca}}$ except for the most heavily doped crystal (CB-1), for which $N_I \simeq 4 \times N_{B_{Ca}}$.

Our model for the variable charge state of B-antisite defects explains, in a natural way, other experimental results. In spite of the fact that weak ferromagnetism has been found in some CaB_6 crystals [1], all our samples were diamagnetic or slightly paramagnetic. In the model we propose, only B^{+2} ions have unpaired electrons, which can—under conditions we specify further below—contribute to the ferromagnetism that is observed in CaB_6. Their density N_1 depends drastically on impurity concentration N_I. This is illustrated in Fig. 4(a), where $N_1/N_{B_{Ca}}$ is plotted as a function of temperature, for various $N_I/N_{B_{Ca}}$ ratios. The curves we have calculated are for $m^* = 0.30m_0$, $N_{B_{Ca}} = 2 \times 10^{19}$, $E_1 = 0.013$ eV, and $E_2 = 0.03$ eV. The drop of N_1 with increasing N_I is striking if $N_I/N_{B_{Ca}} > 1$, especially at low temperatures. We also find that, in a broad temperature range, the Fermi level is pinned between energy E_1 and E_2 if [see inset of Fig. 4(a)] $N_I/N_{B_{Ca}} \simeq 1.0$. Furthermore, electron concentration in the conduction band depends rather weakly on temperature for all $N_I/N_{B_{Ca}}$ ratios [see Fig. 4(b)]. Similar results are obtained for a quite wide range of parameters $N_{B_{Ca}}$, E_1, and E_2.

All of this points to a picture in which a condition $N_I/N_{B_{Ca}} \lesssim 1$ favors significant occupancy of the E_1 levels with the Fermi level close to or at E_1. Then, one can see from Fig. 4(a) that $N_1/N_{B_{Ca}} \gtrsim 0.3$. It follows that a density of 10^{-3} of E_1 defects per unit cell can be reached if $N_{B_{Ca}} \gtrsim 10^{19}$ cm^{-3}. These defects' magnetic moments can therefore lead to ferromagnetism [6]. Moreover, under the condition $N_I/N_{B_{Ca}} \simeq 1$, $n(T)$ does not vary much with N_I. This would explain why ferromagnetic moments—found for lightly doped CaB_6 samples—show no systematic variation with electron doping level [16]. We also note that some schemes for ferromagnetism require a high density of states at the Fermi level, such as a narrow impurity band, in order to satisfy the Stoner criterion [3]. This is what happens in our

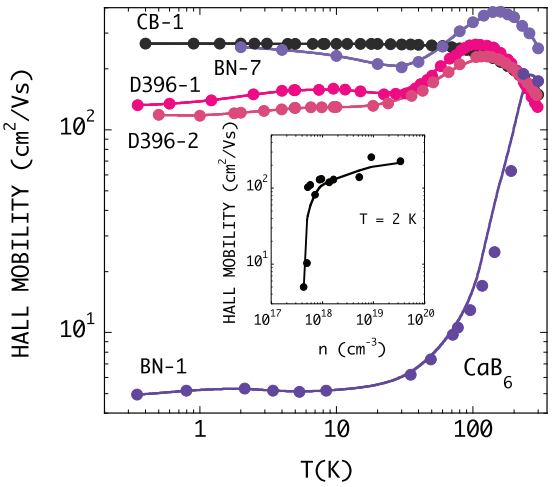

FIG. 5. (Color online) Hall mobility vs temperature for various CaB_6 single crystals. The inset shows Hall mobility vs electron concentration at $T = 2$ K.

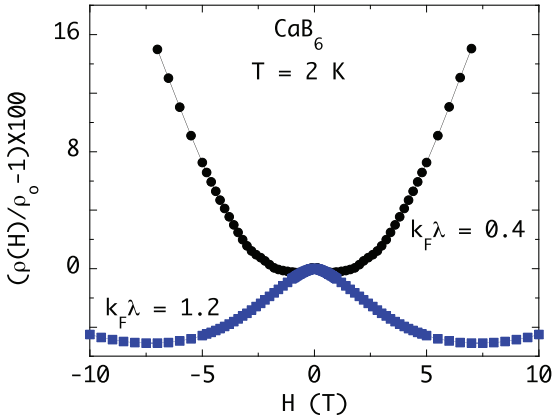

FIG. 6. (Color online) Low–temperature magnetoresistance for two CaB_6 single crystals in different localization regimes.

model. How ferromagnetism arises from this is, however, out of the scope of this paper.

It is worth mentioning that Al substitutional impurities, which can be introduced when samples are grown in an Al flux, would in our model give the same effects as B-antisite defects. However, it has been shown that their concentration in CaB_6 would be negligible for growth under thermal equilibrium conditions [17]. Recent results for a CaB_6 single crystal grown by a liquid Ca–solid B reaction under high temperature and high pressure conditions are in line with this conclusion [18]. The temperature variation of the Hall coefficient reported in Ref. [18] follows the trend of our results although no Al flux had been used in crystal growth. The authors of this report attribute such behavior to a semi-metallic nature of CaB_6. However, their conclusions are at odds with our model and with recent results obtained for electronic conduction in CaB_6 single crystals at high pressure [19]. In particular, electronic transport measurements under hydrostatic pressure and varying temperature would provide complementary information about the defects' nature in alkaline-earth hexaborides. Such measurements are yet very scarce for CaB_6 [19,20] even though exotic high-pressure phases have been found in this system [21].

Finally, we discuss low-field Hall mobility in CaB_6 single crystals. Figure 5 shows how the mobility, obtained from $\mu_H = R_H/\rho$, varies with temperature. For $N_{B_{Ca}}$ in the 10^{18}–10^{19} cm^{-3} range and $N_I \lesssim N_{B_{Ca}}$, μ_H has a maximum at approximately 150 K and drops to a nearly constant value at lower temperatures. In the most doped sample CB-1, for which $N_I > N_{B_{Ca}}$, the Hall mobility is constant for $T \lesssim 100$ K and decreases further on. In the single crystals with low defect density, on the other hand, μ_H drops to quite small values at low temperatures.

Carrier mobilities in a moderately doped semiconductor are usually controlled by electron-phonon scattering and, at lower temperatures, by ionized impurity scattering. A very weak temperature variation of μ_H below $T \lesssim 100$ K, however, points to another contribution to mobility in CaB_6 crystals which is the scattering at neutral impurities. An expression derived by Erginsoy [22] for the mobility limited by this process gives $\mu_{ni} = m^* e^3/(20\epsilon\hbar^3 N_0)$, where ϵ is the dielectric constant, e is the electron charge, and N_0 is the density of neutral scattering centers. Good agreement with experimental values is obtained for $N_0 \simeq 10^{19}$. On the other hand, close to room temperature, the mobility varies as $T^{-3/2}$. From this, we infer it is limited by acoustic lattice vibrations.

In the inset of Fig. 5, μ_H is plotted versus electron concentration at $T = 2$ K. A sharp drop at $n \approx 1 \times 10^{18}$ cm^{-3} corresponds to a metal-insulator transition. Using the Mott relation for the critical concentration, $n_c = (0.26/a_B)^3$, we get $a_B \simeq 26$ Å for the Bohr radius. This is quite close to the estimated value of 15 Å for a_B, using the material parameters of CaB_6 [15,23]. The $k_F\lambda$, where $k_F = (3\pi^2 n)^{1/3}$ is the Fermi wave number and $\lambda = (\hbar/e)k_F\mu$ is the mean free path, is much smaller than 1 for crystals with low electron density, which suggests a strongly localized regime. Most of our samples however are in a weakly localized regime (WLR), for which $k_F\lambda \simeq 1$. The magnetoresistance (MR) of CaB_6 single crystals varies, as shown in Fig. 6, smoothly from positive, for $n < n_c$, to negative values, for $n > n_c$. Diamagnetic shrinking of the wave function leads to a drop of hopping conduction, which in turn, gives the positive magnetoresistance we observe [24]. The negative magnetoresistance in the WLR regime most likely arises from the effects of the magnetic field on the coherence of backscattered electrons [25] and on electron-electron interactions [26]. A detailed discussion of these and other MR data will be published elsewhere [27].

In summary, the variation of the electrical resistivity and of the Hall effect with temperature in CaB_6 single crystals can be consistently explained by a variable charge state of intrinsic defects. These defects are most likely B antisites, as suggested by calculations [11] and in agreement with the high-resolution photoemission study showing the *2p* character of the impurity features in CaB_6 [28]. Our model is also consistent with the presence of a narrow, defect related, impurity band close to the Fermi level. Thus it may indicate the validity of defect-driven intrinsic ferromagnetism in alkaline-earth hexaborides [17,29]. Such mechanism seems to be responsible for ferromagnetic properties of nano–CaB_6 films [30,31].

ACKNOWLEDGMENTS

We acknowledge support from Grant No. MAT2012-38213-C02-01, from the Ministerio de Economía y Competividad of Spain. Additional support from Diputación General de Aragón (DGA-CAMRADS) is also acknowledged. The work at the University of Warwick was supported by Grant No. EP/I007210/1 from EPSRC, UK.

[1] D. P. Young, D. Hall, M. E. Torelli, Z. Fisk, J. L. Sarrao, J. D. Thompson, H. R. Ott, S. B. Oseroff, R. G. Goodrich, and R. Zysler, Nature (London) **397**, 412 (1999).
[2] H. R. Ott, J. L. Gavilano, B. Ambrosini, P. Vonlanthen, E. Felder, L. Degiorgi, D. P. Young, Z. Fisk, and R. Zysler, Physica B **281-282**, 423 (2000).
[3] D. M. Edwards and M. I. Katsnelson, J. Phys.: Condens. Matter **18**, 7209 (2006).
[4] J. D. Denlinger, J. A. Clack, J. W. Allen, G.-H. Gweon, D. M. Poirier, C. G. Olson, J. L. Sarrao, A. D. Bianchi, and Z. Fisk, Phys. Rev. Lett. **89**, 157601 (2002).
[5] K. Giannó, A. V. Sologubenko, H. R. Ott, A. D. Bianchi, and Z. Fisk, J. Phys.: Condens. Matter **14**, 1035 (2002).
[6] Z. Fisk, H. R. Ott, V. Barzykina, and L. P. Gorkov, Physica B **312-313**, 808 (2002).
[7] S. Paschen, D. Pushin, M. Schlatter, P. Vonlanthen, H. R. Ott, D. P. Young, and Z. Fisk, Phys. Rev. B **61**, 4174 (2000).
[8] P. Vonlanthen, E. Felder, L. Degiorgi, H. R. Ott, D. P. Young, A. D. Bianchi, and Z. Fisk, Phys. Rev. B **62**, 10076 (2000).
[9] H. R. Ott, M. Chernikov, E. Felder, L. Degiorgi, E. G. Moshopoulou, J. L. Sarrao, and Z. Fisk, Z. Phys. B **102**, 337 (1997).
[10] T. Morikawa, T. Nishioka, and N. K. Sato, J. Phys. Soc. Jpn. **70**, 341 (2001).
[11] I. J. Kang and C. H. Park, J. Korean Phys. Soc. **49**, S490 (2006).
[12] W. Walukiewicz, Physica B **302-303**, 123 (2001).
[13] W. Shockley and J. T. Last, Phys. Rev. **107**, 392 (1957).
[14] Yu. V. Andreev, K. I. Gelman, I. A. Drabkin, A. V. Matveenko, E. A. Mozhaev, and B. Ya. Molzhes, Moizhes, Fiz. Tekn. Poluprovodn. **9**, 1873 (1975) [Sov. Phys. Semicond. **9**, 1235 (1975)].
[15] H. J. Tromp, P. van Gelderen, P. J. Kelly, G. Brocks, and P. A. Bobbert, Phys. Rev. Lett. **87**, 016401 (2001).
[16] M. C. Bennett, J. van Lierop, E. M. Berkeley, J. F. Mansfield, C. Henderson, M. C. Aronson, D. P. Young, A. Bianchi, Z. Fisk, F. Balakirev, and A. Lacerda, Phys. Rev. B **69**, 132407 (2004).
[17] R. Monnier and B. Delley, Phys. Rev. Lett. **87**, 157204 (2001).
[18] S. Xin, S. Liu, Z. Zhao, J. Yang, B. Xu, Y. Tian, and D. Yu, Sci. China Phys. Mech. Astron. **54**, 1791 (2011).
[19] M. Li, H. Wang, K. Snoussi, L. Li, W. Yang, and C. X. Gao, J. Appl. Phys. **108**, 103710 (2010).
[20] Y. Li, J. Yang, X. Cui, T. Hu, C. Liu, Y. Tian, H. Liu, Y. Han, and C. X. Gao, Phys. Status Solidi B **248**, 1162 (2011).
[21] A. N. Kolmogorov, S. Shah, E. R. Margine, A. K. Kleppe, and A. P. Jephcoat, Phys. Rev. Lett. **109**, 075501 (2012).
[22] C. Erginsoy, Phys. Rev. **79**, 1013 (1950).
[23] C. O. Rodriguez, R. Weht, and W. E. Pickett, Phys. Rev. Lett. **84**, 3903 (2000).
[24] B. I. Shklovskii and A. L. Efros, in *Electronic Properties of Doped Semiconductors* (Springer-Verlag, New York, 1984).
[25] A. Kawabata, J. Phys. Soc. Jpn. **49**, 628 (1980).
[26] B. L. Altshuler and A. G. Aronov, in *Electron-Electron Interactions in Disordered Systems*, edited by M. Pollak and A. L. Efros (North-Holland, Amsterdam, 1985).
[27] J. Stankiewicz and Z. Fisk (unpublished).
[28] K. Maiti, V. R. R. Medicherla, S. Patil, and R. S. Singh, Phys. Rev. Lett. **99**, 266401 (2007).
[29] K. Maiti, Europhys. Lett. **82**, 67006 (2008).
[30] L. S. Dorneles, M. Venkatesan, M. Moliner, J. G. Lunney, and J. M. D. Coey, Appl. Phys. Lett. **85**, 6377 (2004).
[31] G. Zhao, L. Zhang, L. Hu, H. Yu, G. Min, and H. Yu, J. Alloys Compd. **599**, 175 (2014).